Available online at www.sciencedirect.com
ScienceDirect
Journal of the European Ceramic Society 26 (2006) 3509–3514
www.elsevier.com/locate/jeurceramsoc

Structure and mechanical properties of plasma sprayed coatings of titania and alumina

Pavel Ctibor[a,*], Petr Boháč[b], Martin Stranyánek[b], Radim Čtvrtlík[b]

[a] *Institute of Plasma Physics ASCR, Prague, Czech Republic*
[b] *Institute of Physics ASCR, Prague, Czech Republic*

Received 1 October 2005; received in revised form 14 December 2005; accepted 28 December 2005
Available online 20 February 2006

Abstract

The paper concerns the use of traditional and depth-sensing indentation (DSI) for investigation of deposits produced from powders based on conventional and nano-sized particles by plasma spray technology.

Plasma sprayed coatings of titania and alumina were studied. Polished cross-section of each coating was prepared and matrices of nano-indents with Berkovich tip were applied onto both materials to explore local elastic behavior. Applied load was in the range of mN to create indents with the same size scale as the thickness of splats—the main building units of the coating. The hardness value as well as the load/unload curve for each indent was stored. Titania coating was sprayed from a novel type of nanoscale-size powder agglomerated to particles useful for plasma spraying, whereas fused and crushed conventional powder was utilized for alumina spraying and for titania coating used as reference. The effect of annealing on elastic properties of titania was studied as well. The values of elastic parameters as well as the character of the coating inhomogeneity seem to reflect: (i) the composition of material and the fabrication technique and (ii) microstructural differences between coatings that are partly inherited from the feedstock powders. The results of DSI tests are discussed also in comparison with common technique used for the investigation of plasma coatings hardness—Vickers microhardness measurement.

Keywords: Plasma spraying; Optical microscopy; Mechanical properties; TiO_2; Al_2O_3

1. Introduction

1.1. Plasma sprayed coatings

Plasma sprayed coatings are produced by introducing powder particles of the feedstock material into a plasma jet, which melts them and propels towards the substrate. The formation of a coating depends on the interaction between a droplet and the substrate or the previously deposited layers, i.e., spreading of a droplet, the formation of a splat (lamella) and its solidification. The difference in the degree of a splat flattening results in the difference in porosity and its shape as well as distribution, and these factors could affect also the bonding between lamellae. Bonding between lamellae affects markedly the cohesion and elastic properties of the coating. The main spray parameters of the system—feeding distance (i.e., spray gun to feeding point distance) and spray distance (i.e., spray gun to substrate distance) are able to control the majority of the above-mentioned features.

1.2. DSI test and Oliver–Pharr method

The method[1] was introduced in 1992 for measuring hardness and elastic modulus by instrumented indentation techniques and it has been widely adopted and used in the characterization of small-scale mechanical behavior. Its appeal stems largely from the fact that mechanical properties can be determined directly from the indentation load and displacement measurements without the need to image the hardness impression. With high-resolution testing equipment, this facilitates the measurement of the properties at micrometer and nanometer scales. For this reason, the method has become a primary technique for determining the mechanical properties of thin films or small structural features of bulk or thick films. It was originally intended for

* Corresponding author. Tel.: +420 2 66 05 37 27; fax: +420 2 85 86 389.
E-mail address: ctibor@ipp.cas.cz (P. Ctibor).

0955-2219/$ – see front matter © 2006 Elsevier Ltd. All rights reserved.
doi:10.1016/j.jeurceramsoc.2005.12.018

application with sharp, geometrically self-similar indenters like the Berkovich triangular pyramid. There are three important quantities that can be measured from the P–h curves: the maximum load, P_{max}, the maximum indentation depth, h_{max}, and the elastic unloading stiffness, $S = dP/dh$, defined as the slope of the upper part of the unloading curve at the initial point of unloading (also called the contact stiffness). Once the contact area A is determined, the hardness is estimated from: $H = P_{max}/A$. Note that because this definition of hardness is based on the contact area under load, it may deviate from the traditional hardness measured from the area of the residual hardness impression if there is significant elastic recovery during unloading. However, this is generally important only in materials with extremely small values of E/H. Measurement of the elastic modulus follows from its relationship to the contact area and the measured unloading stiffness through the relation:

$$S = \beta \frac{2}{\sqrt{\pi}} E_r \sqrt{A}$$

where β is a correction factor and E_r is the effective elastic modulus defined by

$$\frac{1}{E_r} = \frac{1 - \nu^2}{E} + \frac{1 - \nu_i^2}{E_i}$$

the effective elastic modulus takes into account the fact that elastic displacements occur in both the specimen, with Young's modulus E and Poisson's ratio ν, and the indenter, with elastic constants E_i and ν_i.[1]

1.3. Indentation tests in the research of sprayed ceramic coatings

The depth-sensing indentation test is useful also for brittle material as bulk ceramics. The measurement of the indentation geometry on typical commercial ceramic materials, as compared with typical metallic materials, can be made only with higher scatter and reduced reproducibility, which is caused by the stochastic indentation response.[2] Chipping and cracking is the reason for this scatter of results. The same effect, but even more pronounced, is typical for sprayed ceramic coatings. Here the results reveal the role of microstructural features on the material performance, in particular the critical influence of porosity, splat size and inter-splat cohesion, on the multiple-splat scale wear and indentation behavior of the coatings.[3] Indentation techniques probe microstructure on the size scale of the indenter used and are usually carried out under compression. The scale varies from nanometers, where mechanical properties of materials within a single splat can be studied, through to micrometers.[4] Until the present time, of course, the experience is broader with techniques utilizing less expensive instrumentation, like traditional microhardness measurement.

Plasma sprayed TiO_2 coating using conventional powder exhibits microhardness of about 8.5 GPa.[7] The papers dealing with overall mechanical properties of TiO_2 sprayed using nanopowders as starting material[7,8] enable us to anticipate certain enhancement compared to conventional coatings.

Also the aim of the experiments presented here is to use traditional and depth-sensing indentation for investigation of deposits produced using powders based on conventional and nano-sized particles in plasma spray technology.

2. Experimental

2.1. Selection of conventional powders and sample preparation

Alumina—sample labelled AH (Al_2O_3 + 4.7 wt.%TiO_2 + 1.4 wt.%Fe_2O_3).
Titania—sample labelled MP-1 (TiO_2).

Fused and crushed powders were used as a feedstock. Samples were manufactured using a high-throughput water-stabilized plasma spray system WSP® 500 (Institute of Plasma Physics, Prague, Czech Republic). This system operates at about 160 kW arc power and can process substantial amounts of material per hour. Main spray parameters of this system – feeding distance (i.e., spray gun to feeding point distance) and spray distance (i.e., spray gun to substrate distance) – were maintained as usual when conventional ceramic powders are sprayed. As substrates, flat carbon steel coupons were used. The powder was forced in by compressed air through two injectors. Deposited coating thickness was about 1.5 mm. The sample was investigated as a so-called free-standing body, i.e., without substrate, which was stripped off by the procedure utilizing mismatch in the thermal expansion coefficients.

2.2. Annealed sample production

2.2.1. Titania—sample labeled MP-2 (TiO_2)

Plasma as-sprayed deposit in the form of free-standing body was annealed at 1300 °C with dwell time 1 h. Laboratory furnace with air atmosphere was used. Air atmosphere is helpful to maintain the stoichiometry of the titania sample.

2.3. Selection of powders based on nanoparticles and sample preparation

2.3.1. Titania—sample labeled NP (TiO_2)

TiO_2 powder "Ti NanoCoat VHP TSGP" (Altair Nanomaterials Inc., Reno, NV, USA) was used as a feedstock. The nanometric powder product consists of anatase phase, crystals in the 40-nanometer size range, which are equiaxial in shape. This product exhibits no crystal growth or change of phase when kept in an oxidizing atmosphere at 500 °C for over 24 h (information provided by the powder producer). TSGP (thermal spray grade powder) was prepared from nanometric powder by agglomeration. The enhanced sintering properties of the primary nanoparticles represent a novel approach to this field. Materials produced using this powder as a feedstock offer superior corrosion and abrasion resistance relative to existing commercial products. Several thermal spray companies (including IPP ASCR) are developing and testing advanced nano-sized thermal spray coatings. Testing programs are under way to prove

Table 1
Torch parameters used for WSP spraying

Material	Alumina	Titania
Current (A)	500	500
Power (kW)	160	160
Feeding distance (mm)	24	56
Spray distance (mm)	300	350
Feeding gas	Air	Ar
Powder size (μm)	63–80	45–75

that meta-stable nano-sized particles of ceramic crystals will grow and fuse together when splatted on a metal surface from a plasma spray gun. Initial tests indicate that the coatings result in an impermeable layer, with finer voids and defects than conventional micron-sized powders.

Plasma spray equipment and process was the same as described in the paragraph dealing with conventional powders; near-optimal parameters for each material were found before spraying and are summarized in Table 1.

2.4. Microhardness

The microhardness indentation test was performed using the Hanemann microhardness head mounted on a light microscope (Neophot 2, Zeiss, Germany). A Vickers diamond indenter was employed. The test load applied was 1 N and the holding time remained at 15 s for all tests.

All the indentations were made on polished cross-sections of the coatings. The samples were polished using an identical procedure—fine polishing with diamond paste of 6 and 3 μm grain size and finished with a diamond paste of 1 μm grain size. The distance between indentations was at least five times larger than the diagonal of the largest indentation so as to avoid the effect of stress fields near indentations. The results were the average of 25 readings while indents from various areas of a cross-section for each sample were analyzed.

2.5. Nanohardness and elasticity modulus

Experiments were performed on the NanoTest^{TM} NT600 (Micro Materials, Ltd., Wrexham, UK) device. The setup differs from other devices by the horizontal orientation of the indenter axis. Also gravity-related imperfections in loading procedure are easily avoided. A resolution of 1 μN and 0.1 nm is guaranteed by the producer.[9] All samples have undergone 100 indentations with a calibrated Berkovich indenter. The distance between indents in a matrix 10 × 10 was 20 μm, where the load 100 mN was applied. Loading and unloading time was 20 s when it was performed by a constant speed of 5 mN s^{-1}. The data were adjusted by subtracting the indents whose load–displacement curve was of non-standard shape, namely if subsequent visual control verified the defect in the structure at the point of indentation. This subtraction leads to discrimination against results that would be useless for hardness and elasticity modulus calculation using the Oliver–Pharr approach but are not atypical for the overall material properties. So, the results presented here should be seen as local elastic properties of the coating. Calculation of nanohardness and H_{ind} and effective elasticity modulus E_r were performed according to the Oliver and Pharr method.[1]

2.6. Microstructural observation and porosity measurement

Porosity was determined on light microscopy images of cross-sections via image analysis software (Lucia G, Laboratory Imaging Ltd., Czech Republic). Images were taken before indentation and 10 randomly selected images of each sample were analyzed. Presented images of nanoindents were taken by the same equipment.

3. Results and discussion

Table 2 summarizes the results of traditional Vickers (HVm) and nanohardness (H-dsi) testing on conventional (MP-1), annealed conventional (MP-2) and nano-powder (NP) titania coatings. Elasticity modulus E_r and porosity results are added.

Sample MP-1 exhibits bimodal distribution of nanohardness values. One maximum is at 11.9 GPa and the second one at 7.6 GPa. Their bimodal character is attributed to the presence of two different predominant crystal orientations in the deposit. We suppose similar microstructural effect like in,[12] but deeper investigation is still under way.

The homogeneity of the nano-powder deposit NP is better than the homogeneity of the conventional deposit MP-1, which is visible from the character of the nanohardness histogram Fig. 1 and is reflected also in the size of standard deviation bars in Fig. 2. The scatter of the data is lower for nano-powder deposit NP, and the distribution in Fig. 1 is wider for conventional coating. Fig. 3 shows histograms of microhardness for titania samples. Annealed sample MP-2 is the best, which agrees with well-established knowledge that annealing improves

Table 2
Results on titania samples

Sample	H (GPa)			Modulus E_r (GPa)		Porosity (%)
	Vickers	Nanohardness				
NP	12.5 ± 1.2	10.0 ± 1.8		185.1 ± 22.4		8.7
MP-1	13.0 ± 1.6	11.9 ± 1.1	7.6 ± 1.2	209.5 ± 22.8	155.3 ± 24.1	7.0
MP-2	13.4 ± 1.1	11.8 ± 0.9		197.7 ± 20.1		4.9

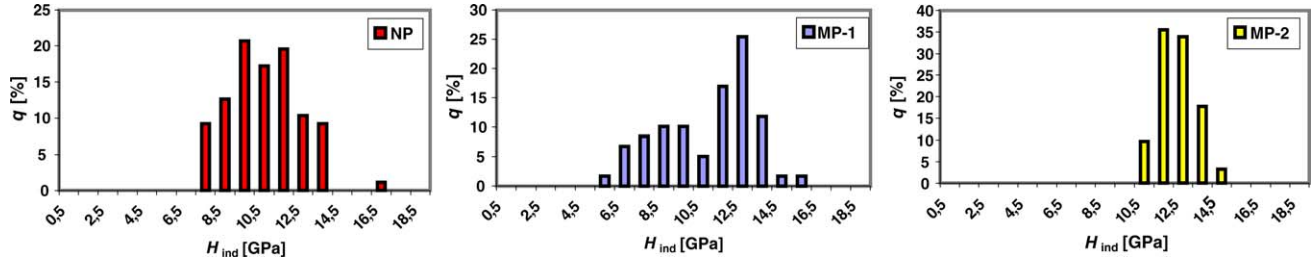

Fig. 1. Histograms of nanohardness for titania samples: NP (left), MP-1 (middle) and MP-2 (right).

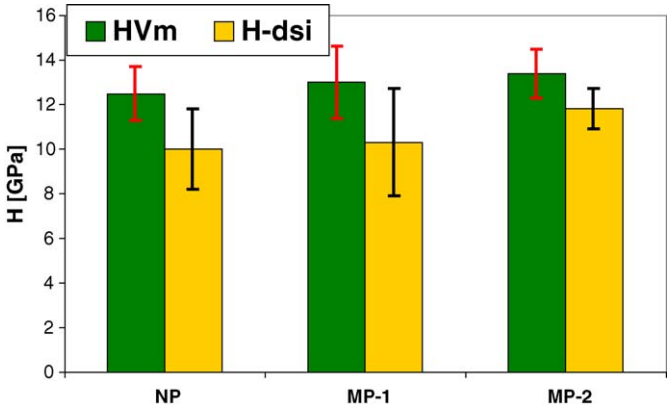

Fig. 2. Comparison of HVm and H-dsi average hardness for titania samples: NP (left), MP-1 (middle) and MP-2 (right). Standard deviation bars are added.

Table 3
Microhardness of alumina determined using (traditional HVm) Vickers indenter, load 1 N, 15–20 valid indentations

Microhardness (GPa)	Comment
21.2 ± 0.2	Material of best quality regarding hardness test[5]
19.9 ± 0.9	Ceramics with low porosity, fine grained, single-phase[5]
15.3 ± 2.0	Ceramics with medium porosity, medium grain size, multi-phase[5]
16.8 ± 0.7	Plasma sprayed coating, multi-phase AH[6]

microstructure of plasma sprayed deposits and it is reflected in improved mechanical properties. Fig. 4 also documents that microstructural features like lamellae and voids are finer in scale on the sample NP than on the MP-1 and the lamellar character disappeared on the MP-2 sample to become bulk-like after annealing.

Fig. 5 gives nine DSI indents from the matrix 10×10 at sample MP-1 and corresponding data placed in the matrix with the same coordinates. Please note the indent No. 93 (bold data) is placed on a crack and hence its data are extraordinarily low.

Fig. 6 shows a histogram of nanohardness for alumina sample. Compared to titania samples, Fig. 1, alumina has a very wide distribution. Here the mean value is 13.8 ± 3.1 GPa; the average is easily the highest from all samples, but the same holds for its standard deviation as well. Alumina is one of the hardest commonly sprayed ceramic materials. In Table 3 microhardness results with references are listed. 'Single-phase' in Table 3 means alpha phase and 'multi-phase' means a mixture of alpha and gamma phases. Well-known facts are that the alpha phase is harder than gamma and that plasma spraying leads predominantly to gamma phase formation. The slightly bimodal character of the distribution (see Fig. 6) could mean the separation of two existing phases, but to reveal the crystalline structure in such a small area as that of a single nano-indent is a serious problem. Spatial resolution of X-ray diffraction techniques is not satisfactory for investigation of splat-to-splat variation of phase composition on coating section.

Elastic modulus calculated from the depth-sensing indentation is 167.9 ± 28.3, which is of lower value and higher standard deviation compared to all titania samples. Fig. 7 shows the only prematurely solidified particle (PSP, in former work[10] less correctly labeled 'unmelted') found at a spot of nanoindentation. The PSPs are considered to have been spheroidized in the plasma plume during plasma spraying, but to have

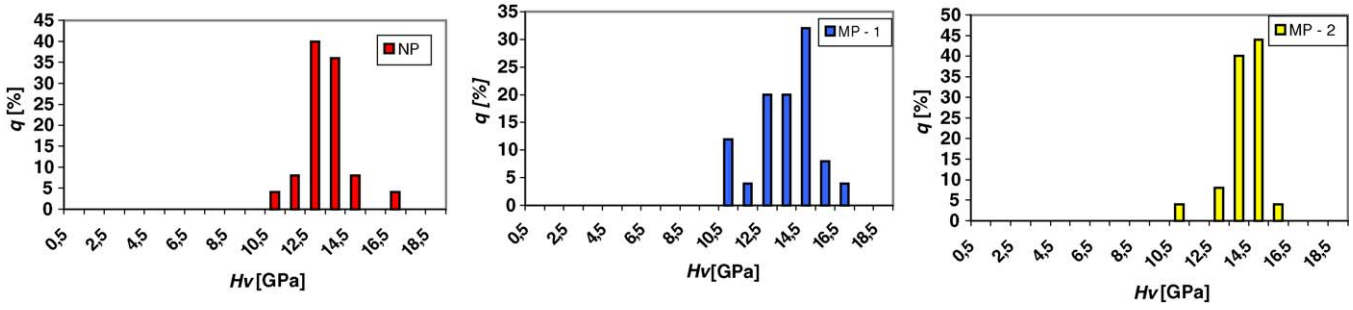

Fig. 3. Histograms of microhardness for titania samples: NP (left), MP-1 (middle) and MP-2 (right).

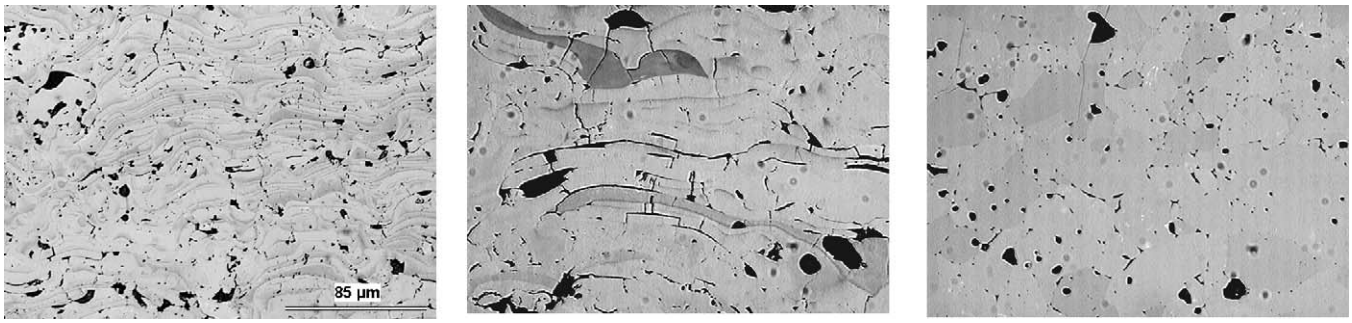

Fig. 4. Light micrographs of titania samples: NP (left), MP-1 (middle) and MP-2 (right). Magnification is the same in all instances.

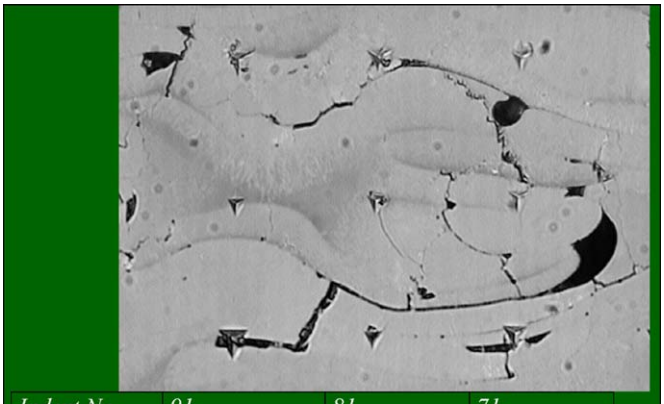

Indent No.	*91*	*81*	*71*
H-dsi [GPa]	6.87	10.15	12.24
E_r	166.0	229.9	221.8
Indent No.	*92*	*82*	*72*
H-dsi [GPa]	8.77	10.77	11.09
E_r	151.0	194.5	173.6
Indent No.	*93*	*82*	*73*
H-dsi [GPa]	**4.65**	9.77	11.29
E_r	**132.0**	186.2	194.8

Fig. 5. Nine DSI trianglular indents (matrix 3 × 3; one vertex steers down) from the matrix 10 × 10 in sample MP-1 and corresponding data.

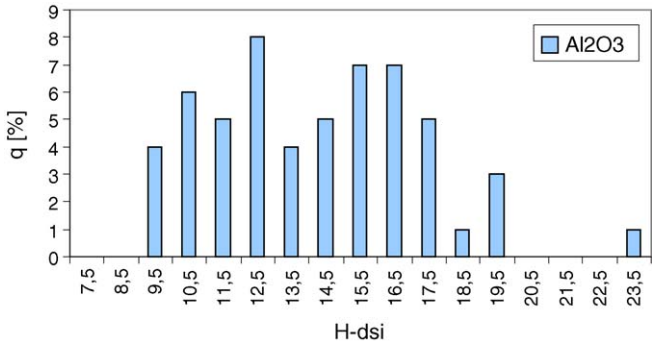

Fig. 6. Histogram of nanohardness for alumina sample.

been cooled below the melting point before reaching the substrate. Such particles are embedded in the lamellar coating as previously solidified, i.e., of approximately globular shape.[10] This one corresponds to indent No.48 and has a hardness of 23.5 GPa and elasticity modulus of 210.1 GPa. All those values are the best among entire matrix of indents, which fact is in concordance with the existence of the alpha or delta phase in alumina particles collected in flight without impact on substrate.[11]

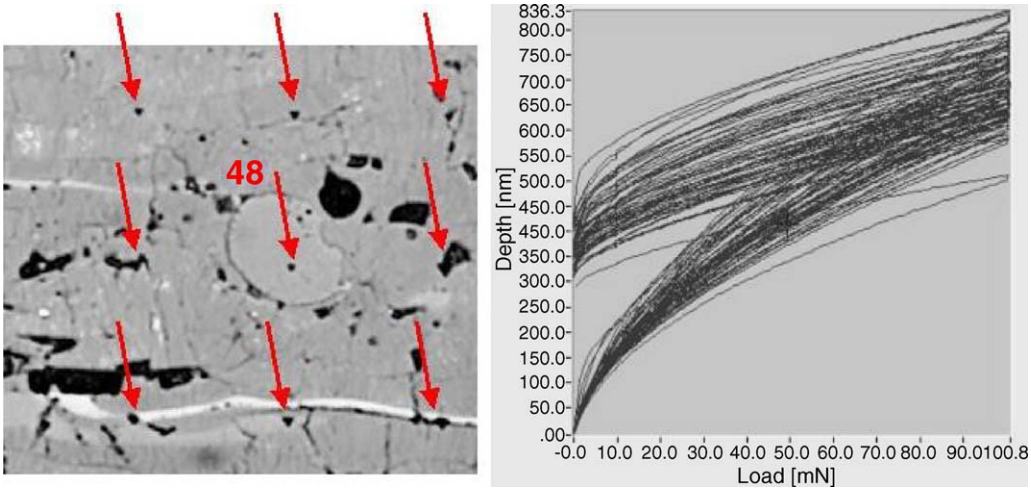

Fig. 7. Unmelted particle around indent No.48 (left) and all load/depth curves of AH sample (right). The curve belonging to the indent No.48 has the lowest depth at load 100.8 mN.

4. Conclusions

Advanced nano-powder titania deposit NP has improved microstructure compare to conventional powder-based deposit MP-1 and also scatter of mechanical properties is reduced. This fact is more easily detectable by the depth sensing indentation than by traditional Vickers microindentation measuring microhardness. Although improvement of mean values is not attained by NP, annealed sample MP-2 exhibits mild improvement of all studied parameters compared to as-sprayed samples.

Alumina, as expected, exhibits high average hardness but the values are more dispersed and the coating contains a relatively high amount of 'weak-points'.

When large-area deposits are produced, the use of nano-powder based feedstock reduces the probability of the presence of serious defects, the structure is more homogeneous and a higher reliability of the coating in service seems to be more easily attainable. To resolve those aspects of the microstructure, depth-sensing nano-indentation is advantageous compared to the traditional microhardness measurement.

Acknowledgments

The authors wish to thank to Altair Nanomaterials Inc., 204 Edison Way, Reno, NV 89502, USA, for providing the TiO_2 powder "Ti NanoCoat VHP TSGP".

Plasma spraying and microhardness measurement were sponsored by the Academy of Science of the Czech Republic under project AV0 Z 20430508.

Depth-sensing indentation was supported by Institutional Research Plan No. AV0Z10100522 and by the project of AS CR No. 1QS100100563.

References

1. Oliver, W. C. and Pharr, G. M., Measurement of hardness and elastic modulus by instrumented indentation: Advances in understanding and refinements to methodology. *J. Mater. Res.*, 2004, **19**(1), 3–20.
2. Ullner, C., Beckmann, J. and Morrel, R., Instrumented indentation test for advanced technical ceramics. *J. Eur. Ceram. Soc.*, 2002, **22**, 1183–1189.
3. Hawthorne, H. M., Ericson, L. C., Ross, D., Tai, H. and Troczynski, T., The microstructural dependence of wear and indentation behaviour of some plasma-sprayed alumina coatings. *Wear*, 1997, **203–204**, 709–714.
4. Li, Y. and Khor, K. A., Mechanical properties of the plasma-sprayed Al_2O_3–$ZrSiO_4$ coatings. *Surf. Coat. Technol.*, 2002, **150**, 143–150.
5. Ullner, C. *et al.*, Hardness testing on advanced technical ceramics. *J. Eur. Ceram. Soc.*, 2000, **21**, 439–451.
6. Ctibor, P. et al., Improvement of mechanical properties of Alumina and Zirconia plasma sprayed coatings induced by laser after-treatment. In *Proceedings of International Thermal Spray Conference 2005*. Basel, Switzerland, 1183–1186.
7. Ibrahim, A. and Berndt, C.C., Fatigue and mechanical properties of nanostructured vs. conventional titania (TiO2) coatings. In *Proceedings of International Thermal Spray Conference 2005*. Basel, Switzerland, pp. 855–859, in press.
8. Lima, R.S. and Marple, B.R., Nanostructured and conventional titania coatings for abrasion and slurry-erosion resistance sprayed via APS, VPS and HVOF. In *Proceedings of International Thermal Spray Conference 2005*. Basel, Switzerland, pp. 552–557.
9. Beake, B. D. *et al.*, *Micro Materials NanoTest User Manual*. Micro Materials Ltd., Wrexham, 2004, p. 96.
10. Ctibor, P., Roussel, O. and Tricoire, A., Unmelted particles in plasma sprayed coatings. *J. Eur. Ceram. Soc.*, 2003, **23**, 2993–2999.
11. Chraska, P., Dubsky, J., Neufuss, K. and Pisacka, J., Alumina-base plasma sprayed materials I. *J. Therm. Spray Technol.*, 1997, **6**(3), 320–326.
12. Zhang, J. and Xu, K., Valence electron structure analysis of crystalline orientation in plasma-sprayed TiO_2 coatings. *Appl. Surf. Sci.*, 2004, **221**, 1–3.